Title

Chemical and Pb isotope composition of phenocrysts from bentonites constrains the chronostratigraphy around the Cretaceous-Paleogene boundary in the Hell Creek region, Montana

Journal

Geochemistry Geophysics Geosystems, 16(8)

ISSN

1525-2027

Authors

Ickert, Ryan B
Mulcahy, Sean R
Sprain, Courtney J
et al.

Publication Date

2015-08-01

DOI

10.1002/2015gc005898

Peer reviewed

AGU PUBLICATIONS

Geochemistry, Geophysics, Geosystems

RESEARCH ARTICLE
10.1002/2015GC005898

Key Points:
- Chemical and Pb isotopic compositions of feldspars identify KPB tephra
- Multiple unique tephra can be traced across the basin
- The results provide a better stratigraphic framework around the terrestrial KPB

Supporting Information:
- Supporting Information S1
- Table S1

Correspondence to:
R. B. Ickert,
Ryan.Ickert@gmail.com

Citation:
Ickert, R. B., S. R. Mulcahy, C. J. Sprain, J. F. Banaszak, and P. R. Renne (2015), Chemical and Pb isotope composition of phenocrysts from bentonites constrains the chronostratigraphy around the Cretaceous-Paleogene boundary in the Hell Creek region, Montana, *Geochem. Geophys. Geosyst.*, *16*, 2743–2761, doi:10.1002/2015GC005898.

Received 7 MAY 2015
Accepted 28 JUL 2015
Accepted article online 1 AUG 2015
Published online 21 AUG 2015

Chemical and Pb isotope composition of phenocrysts from bentonites constrains the chronostratigraphy around the Cretaceous-Paleogene boundary in the Hell Creek region, Montana

Ryan B. Ickert[1,2], Sean R. Mulcahy[2], Courtney J. Sprain[1,2], Jessica F. Banaszak[1,2,3], and Paul R. Renne[1,2]

[1]Berkeley Geochronology Center, Berkeley, California, USA, [2]Department of Earth and Planetary Science, University of California, Berkeley, California, USA, [3]School of the Environment, Washington State University, Pullman, Washington, USA

Abstract An excellent record of environmental and paleobiological change around the Cretaceous-Paleogene boundary is preserved in the Hell Creek and Fort Union Formations in the western Williston Basin of northeastern Montana. These records are present in fluvial deposits whose lateral discontinuity hampers long-distance correlation. Geochronology has been focused on bentonite beds that are often present in lignites. To better identify unique bentonites for correlation across the region, the chemical and Pb isotopic composition of feldspar and titanite has been measured on 46 samples. Many of these samples have been dated by $^{40}Ar/^{39}Ar$. The combination of chemical and isotopic compositions of phenocrysts has enabled the identification of several unique bentonite beds. In particular, three horizons located at and above the Cretaceous-Paleogene boundary can now be traced—based on their unique compositions—across the region, clarifying previously ambiguous stratigraphic relationships. Other bentonites show unusual features, such as Pb isotope variations consistent with magma mixing or assimilation, that will make them easy to recognize in future studies. This technique is limited in some cases by more than one bentonite having compositions that cannot be distinguished, or bentonites with abundant xenocrysts. The Pb isotopes are consistent with a derivation from the Bitterroot Batholith, whose age range overlaps that of the tephra. These data provide an improved stratigraphic framework for the Hell Creek region and provide a basis for more focused tephrostratigraphic work, and more generally demonstrate that the combination of mineral chemistry and Pb isotope compositions is an effective technique for tephra correlation.

1. Introduction

Altered silicic tephras (bentonites) interbedded with lignites and clastic deposits in terrestrial strata near the Cretaceous-Paleogene boundary (KPB) in the Hell Creek region of Montana (Figure 1) have yielded important data concerning the age of the KPB and the tempo of related faunal and floral events [*Renne et al.*, 2013; *Sprain et al.*, 2014]. This region has provided a wealth of information about terrestrial biospheric change across the KPB [e.g., *Wilson*, 2005, 2014], yet only recently has the potential for placing these events in a high-resolution time scale been realized.

Early dating efforts [*Folinsbee et al.*, 1963; *Baadsgaard and Lerbekmo*, 1980; *Baadsgaard et al.*, 1988, 1993] focused on a single bentonite stratigraphically near the KPB. Subsequent recognition of sanidine-bearing bentonites at various levels above the KPB led to a more comprehensive $^{40}Ar/^{39}Ar$ study [*Swisher et al.*, 1993] in which bentonites from multiple stratigraphic sections were dated to obtain a regional chronostratigraphy of the early Paleogene Tullock Member of the Fort Union Formation. The work of *Swisher et al.* [1993] was then refined and expanded in scope by *Renne et al.* [2013], *Moore et al.* [2014], and *Sprain et al.* [2014], who dated additional bentonites and laid the groundwork for a regional chronostratigraphic framework with a potential age resolution of ca. 10 ka.

Bentonites in the region are predominantly found within lignite beds that have provided the basis for regional stratigraphic subdivisions of the Tullock Member. The extent to which the lignites identified by

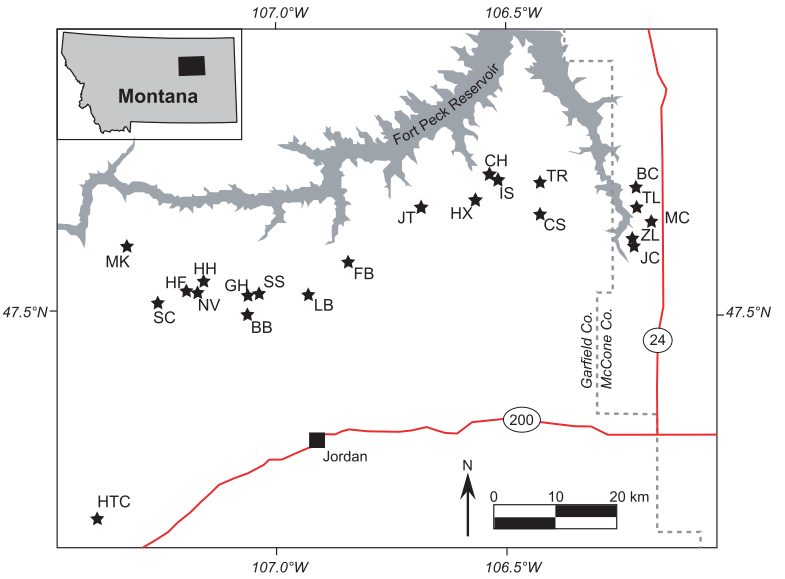

Figure 1. Location of the Hell Creek region within Montana (inset) and the localities referred to in the text within the Hell Creek region, modified from *Sprain et al.* [2014]. HTC = Horsethief Canyon; MK = McKeever Ranch; SC = Snow Creek Road; HF = Hauso Flats; NV = Nirvana; HH = Hell Hollow; GH = Garbani Hill; BB = Biscuit Butte; SS = Saddle Section; LB = Lerbekmo (Hell Creek Road Locality); FB = Flag Butte; JT = Jared's Trike; HX = Haxby Road; CH = Cliffhanger; IS = Isaac Ranch; CS = Constenius; TR = Thomas Ranch; BC = Bug Creek; TL = Tonstein Lignite; MC = McGuire Creek; ZL = Z-line; JC = Jack's Channel.

previous workers are isochronous and can be considered chronostratigraphic units is uncertain, particularly between eastern and western extremities of the region (see discussion by *Sprain et al.* [2014]). *Sprain et al.* [2014] estimated that at least 40 distinct bentonites occur in the 65 m thick Tullock Member, which is bracketed by bentonites dated at 66.043 ± 0.043 and 64.866 ± 0.047 Ma (1σ, here and elsewhere, the uncertainties include systematic uncertainties associated with decay rates and flux monitors), indicating a mean recurrence interval of ~29 ka for tephra deposition. Much higher frequencies are locally indicated; thus, these new criteria for distinguishing individual bentonites can potentially provide chronostratigraphic markers with much greater temporal resolution than even the ± 10 ka best case afforded by $^{40}Ar/^{39}Ar$ dating.

A number of techniques have been developed to fingerprint and correlate tephra [cf. *Lowe*, 2011] with chemical composition of glass (quenched melt) being the most widely used material for correlation [e.g., *Smith and Westgate*, 1968; *Borchardt et al.*, 1971, 1972; *Brown*, 1982; *Clark et al.*, 2003; *Ukstins Peate et al.*, 2005]. Glasses are particularly useful because they have a wide and continuous range of compositions and are not constrained by a fixed stoichiometry. Unfortunately, glass readily alters to secondary minerals and is therefore rare in older tephras, generally limiting glass-based tephrostratigraphy to Late Cenozoic deposits.

Because glass is not preserved in Hell Creek bentonites, we combine feldspar and titanite mineral chemistry with the Pb isotopic composition of alkali feldspars to correlate a regional tephra. We are able to demonstrate the presence of unique, regionally extensive bentonites that extend the geochronological results and enhance the chronostratigraphic framework. We also characterize a number of other bentonite beds, providing a chemical and isotopic framework for future studies.

2. Geology of the Williston Basin

The Hell Creek region is in the northwestern Williston basin, an intracratonic basin that has been a major depositional center since the Ordovician [*Fowler and Nisbet*, 1985; *Kent and Christopher*, 1994], though in the Cretaceous was part of the larger Western Interior Seaway, extending from the Beaufort sea to the Gulf of Mexico. Within the Hell Creek region, the Hell Creek Formation and the Tullock Member of the Fort Union Formation bracket the Cretaceous-Paleogene boundary (KPB). Correlative units in the eastern and northern portions of the Williston basin include the Hell Creek Formation and Ludlow Member of the Fort Union Formation in North and South Dakota, and the Frenchman and Ravenscrag Formations in Canada [*Hartman*, 2002; *Hartman et al.*, 2014]. These units formed as prograding wedges of clastic Laramide sediment that were deposited during the retreat of the Bearpaw Sea [*Fastovsky*, 1987]. These units were deposited in fluvial systems and consists largely of channel and crevasse splay sandstones and associated siltstone, mudstone, and lignite (coal) floodplain deposits [*Gill and Cobban*, 1973; *Cherven and Jacob*, 1985; *Fastovsky and*

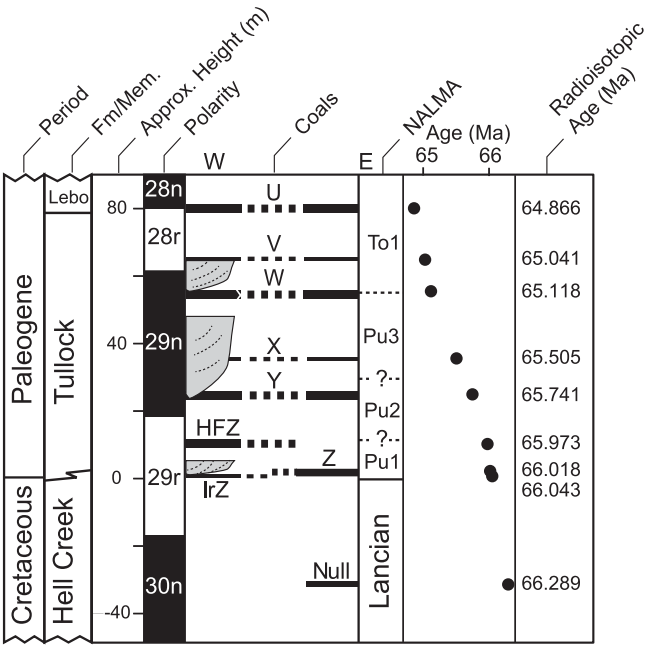

Figure 2. Composite stratigraphic column for the Hell Creek region. NALMA: North American Land Mammal Ages (modified from *Sprain et al.* [2014]).

Dott, 1986]. Late Cretaceous and early Paleogene marine deposits do not occur in the Western portion of the Williston basin, the location of this study, although the occurrence of marine dinoflagellates near the KPB at Flag Butte (FB, Figure 1) [*Moore et al.*, 2014] suggests qualitative proximity to the coastline.

The formational contact between the Hell Creek and Fort Union formations around the Williston basin is roughly near the KPB. Due to an increased hydraulic flux and rise in water table around KPB time, there is a prevalence of variegated beds and organic deposits in the Fort Union Formation compared to the Hell Creek. The formational contact is thus defined at the base of the first laterally persistent lignite, above the highest in situ nonavian dinosaur remains [*Calvert et al.*, 1912; *Brown*, 1952; *Archibald et al.*, 2010; *Hartman et al.*, 2014; *Moore et al.*, 2014]. Recent work has shown that the formational contact (as defined above) throughout the Williston basin, including the Hell Creek region, is diachronous, ranging over several tens of ka [*Sprain et al.*, 2014]. The diachronous nature of the contact thus represents a gradual paleoenvironmental change associated with the first appearance of regionally extensive lignite [*Sprain et al.*, 2014].

In the Hell Creek region, the lignite that defines the formational contact between the Hell Creek Formation and the Tullock Member of the Fort Union Formation is named the Z coal. Stratigraphically higher lignites are named using successive letters in reverse alphabetical order [*Collier and Knechtel*, 1939], as shown schematically in Figure 2. Previous workers generally refer to these lignites as "coals," which is a more general term but a usage that we follow here. The base of the U coal marks the top of the Tullock Member and the base of the Lebo Member of the Fort Union Formation. A few named coals depart from this alphabetical naming scheme including the Null coal, the only well-developed lignite identified within the Hell Creek Formation, and coals in the Z-coal complex including the IrZ, MCZ, and HFZ coals. Despite the general stratigraphic order of successive lignites they are likely not continuous units but rather a series of lenses at roughly similar stratigraphic positions [*Collier and Knechtel*, 1939; *Lofgren*, 1995; *Sprain et al.*, 2014]. Within the Hell Creek region, numerous bentonite (altered volcanic tephra) beds and laminae are present with these lignite beds. The bentonite beds are only rarely preserved outside of the lignites. Little is known about the source of the bentonites or their broader correlation. There are none reported from further east in the basin, in North Dakota, and although some have been found in Saskatchewan, little is known about them.

In this region the KPB is variably defined, but typically characterized by the highest appearance of in situ nonavian dinosaur fossils [*Clemens and Hartman*, 2014; *Hartman et al.*, 2014; *Moore et al.*, 2014] or the lowest occurrence of unreworked Paleocene pollen [*Bercovici et al.*, 2009], and associated with a -1.5 to $-2.8‰$ carbon isotope anomaly [*Arens and Jahren*, 2000, 2002; *Arens et al.*, 2014] and the impact claystone and iridium anomaly, which frequently contains shocked quartz and glass spherules [*Bohor et al.*, 1984; *Bohor*, 1990; *Smit*, 1990]. The KPB is not always coincident with the Hell Creek/Fort Union contact. In the western portion of the Hell Creek region, the Z coal is often associated with an Ir anomaly and impact claystone at or near the base, making the KPB and the formational contact coincident. Z coals with this characteristic are usually referred to as the IrZ coal. However, in the eastern region, the Z coal can be found above Paleocene fossils [*Lofgren*, 1995] and $^{40}Ar/^{39}Ar$ dating has demonstrated that bentonite in the eastern Z coal is resolvably

younger than bentonite in the IrZ coal [*Sprain et al*., 2014]. Thus far, the Ir anomaly has not been found in the eastern area.

2.1. Bentonite Petrology and Mineralogy

Bentonite beds in the Hell Creek region are almost exclusively found within lignite horizons, presumably because preservation was enhanced by the low energy, swamp-like depositional environment. The bentonites are present as layers 0.1 cm to (rarely) 10 cm thick, are typically beige or pinkish in color, and are often laterally discontinuous at the scale of several meters. The stratigraphic context of the samples is shown in Figure 3 and their locations, ages, and petrology are described in Table 1. *Sprain et al*. [2014] provide additional details about field characteristics of some of the bentonite beds that have been dated by $^{40}Ar/^{39}Ar$. Further details are provided in the supporting information.

Sanidine is the only primary igneous mineral ubiquitously preserved in the bentonites. Plagioclase is present in some, but is variably altered. Titanite is notably common, particularly in bentonites of the Null, MCZ, and Y coals, though apatite is generally absent. Biotite (or secondary pseudomorphs of it) and pseudomorphs of beta quartz are present in a few units. Most units sampled contain zircon, but the U-Pb isotopic systematics of this phase in most units sampled indicate pervasive inheritance [*Mitchell*, 2014]. The grains of feldspar and titanite analyzed were all in the 177–420 μm in size.

The matrix of all the bentonites is composed of secondary minerals dominated by clay, but also includes gypsum and carbonate minerals. The clays presumably formed at the expense of original glass shards, whose pseudomorphs are clearly visible in some samples [*Sprain et al*., 2014]. No primary glass has been observed in any of the bentonites, thus the whole-rock chemistry is clearly not expected to reflect primary igneous composition. Accordingly, we used electron probe microanalysis of relict igneous phases (sanidine and titanite, and rarely, plagioclase) in combination with Pb isotope composition of sanidine to characterize the bentonites.

3. Methods

3.1. EPMA Measurements

Electron probe microanalysis (EPMA) of feldspar and titanite was conducted with a Cameca SX-51 in the Department of Earth and Planetary Science at the University of California, Berkeley. Data acquisition, analysis, and correction procedures were conducted with the software Probe for EPMA. Analyses for both phases and the full analytical details are given in the supporting information.

3.2. Pb Isotope Compositions and Tephrochronology

Variability in Pb isotope compositions (ICs) is a function of their source age and history of U-Th-Pb fractionation (e.g., their time-integrated U/Pb and Th/Pb). Unlike other radiogenic isotope systems (e.g., ^{87}Rb-^{86}Sr, ^{147}Sm-^{143}Nd, and ^{176}Lu-^{176}Hf) there are three unique compositional vectors that can be exploited, yielding a wide possible range in Pb composition space. Use of this technique to fingerprint volcanic deposits in tephrochronology has been limited [*Hemming and Rasbury*, 2000; *Ukstins Peate et al*., 2003; *Westgate et al*., 2011].

Lead isotope data from single volcanic fields suggest that there are commonly large variations between eruptive centers, with variations in $^{206}Pb/^{204}Pb$ that are larger than 1% for eruptive products within the Yellowstone, Snake River Plain, and San Juan volcanic fields [*Lipman et al*., 1978; *Doe et al*., 1982]. These results suggest that there may be enough isotopic distinction between eruptions that are closely spaced in time that the Pb ICs may provide unique fingerprints of closely related tephra.

We have used laser-ablation multicollector inductively coupled plasma mass spectrometry (LA-MC-ICPMS) applied to single crystals of alkali-feldspars (sanidine and anorthoclase) to characterize the Pb IC of the juvenile component of the tephra. This approach has several advantages over bulk (solution) analyses [e.g., *Hemming and Rasbury*, 2000] and targeting other materials such as glass [e.g., *Ukstins Peate et al*., 2003; *Westgate et al*., 2011] including (1) K-feldspar (particularly sanidine) is the mineral used for high-precision $^{40}Ar/^{39}Ar$ geochronology in many tephras, directly linking the compositional measurements to geochronological results. (2) Lead is much more compatible in K-feldspar than U and Th and therefore does not require a correction for radiogenic ingrowth [*Sinha*, 1969; *Ludwig and Silver*, 1977; *Housh and Bowring*, 1991]. (3) Measurements by laser ablation require very little sample preparation and are relatively rapid—crystals

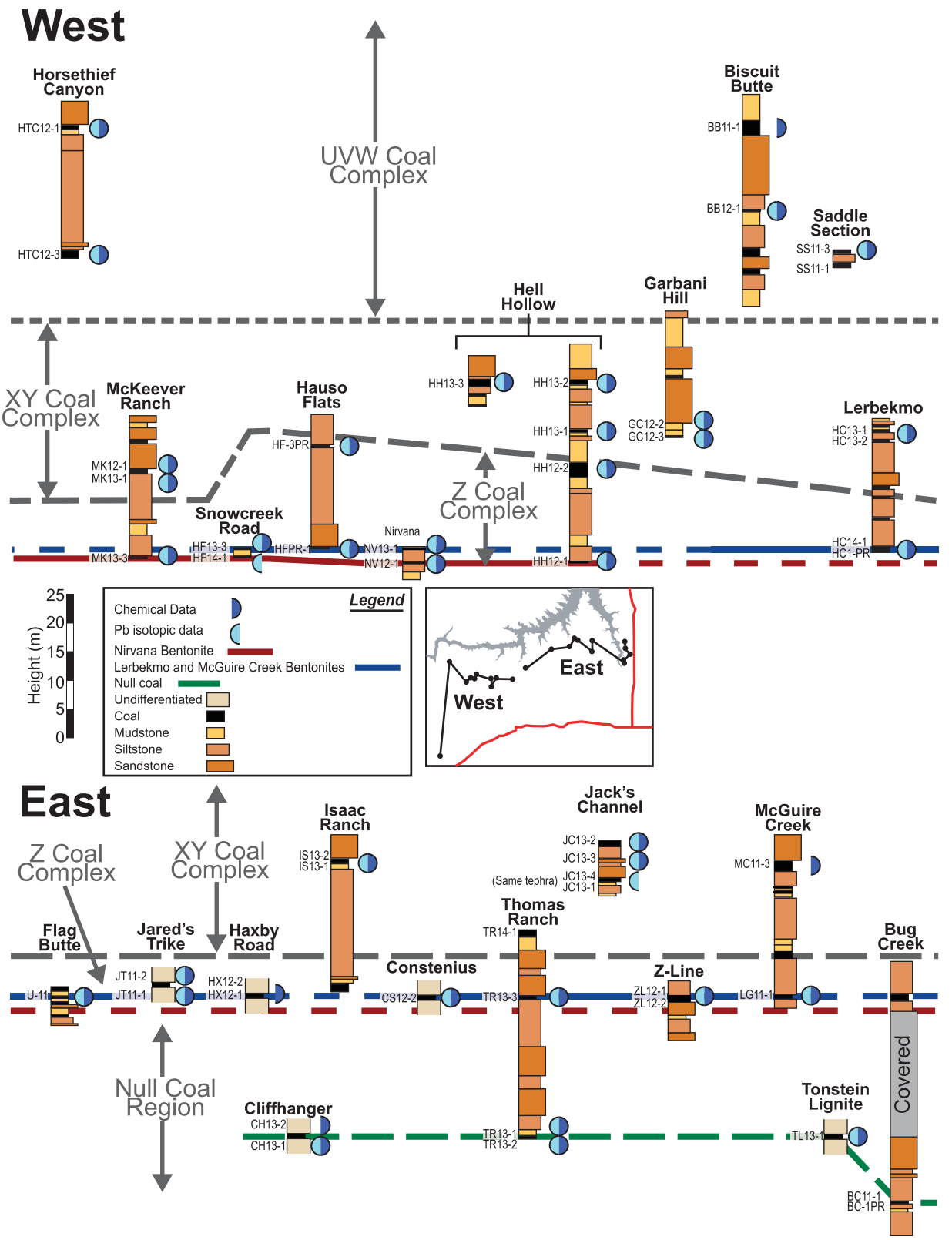

Figure 3. Stratigraphic context of the Hell Creek region bentonite samples. The general stratigraphic range at which lithostratigraphically defined lignite beds are found are indicated with dashed lines and arrows, however these are only approximate and do not represent discrete stratigraphic horizons. Note that the thickness of these ranges is not always constant across the basin. Although not recognized in the eastern portion of the Hell Creek region, the Nirvana bentonite is projected to this region based on its stratigraphic level where both the Nirvana and the Lerbekmo and/or McGuire Creek bentonite are found.

Table 1. Mineralogy Location, and Ages of Bentonite Samples

Sample	Coal-(Bentonite)	Age (Ma)[a]	Xenocrysts[a]	Quartz	Plagioclase	Biotite	Titanite	Latitude (N)	Longitude (W)
BC-1PR/BC11-1	Null	66.289 ± 0.051	120/174	X	X			47°40′48.60″N	106°12′49.56″W
CH13-1	Null			X				47°40′47.76″N	106°30′18.24″W
CH13-2	Null			X				47°40′47.76″N	106°30′18.24″W
TL13-1	Null			X			X	47°38′41.46″N	106°12′50.70″W
TR13-1	Null			X			X	47°39′52.98″N	106°25′39.12″W
TR13-2	Null			X	X		X	47°39′52.98″N	106°25′39.12″W
HF-1PR	IrZ-(Nirvana)	66.043 ± 0.011	7/285	X			X	47°31′43.92″N	107°12′30.78″W
HH12-1	IrZ-(Nirvana)	66.061 ± 0.039	1/71	X	X			47°32′3.60″N	107°10′22.14″W
MK13-3	IrZ-(Nirvana)				X			47°35′37.08″N	107°19′39.60″W
NV12-1	IrZ-(Nirvana)	66.035 ± 0.033	1/56	X	X			47°31′37.14″N	107°11′10.98″W
HF14-1	IrZ-(Nirvana)			x	x			47°30′57.06″N	107°14′22.80″W
HC-2PR	MCZ-(McGuire Creek)	66.019 ± 0.021	0/70		X			47°31′35.58″N	106°56′23.82″W
HF13-3	MCZ-(McGuire Creek)				X	X		47°30′57.06″N	107°14′22.80″W
HX12-1	MCZ-(McGuire Creek)	66.002 ± 0.033	1/94	X				47°38′49.80″N	106°33′37.14″W
JT11-1	MCZ-(McGuire Creek)			X				47°37′46.60″N	106°37′32.10″W
JT11-2	MCZ-(McGuire Creek)			X	X		X	47°37′46.60″N	106°37′32.10″W
LG11-1	MCZ-(McGuire Creek)	66.022 ± 0.038	0/72	X	X		X	47°37′47.50″N	106°10′12.40″W
NV13-1	MCZ-(McGuire Creek)			X			X	47°31′37.14″N	107°11′10.98″W
TR13-3	MCZ-(McGuire Creek)			X	X		X	47°40′0.30″N	106°25′32.88″W
ZL12-2	MCZ-(McGuire Creek)	65.998 ± 0.044	1/89		X	X		47°36′37.26″N	106°12′37.74″W
CS12-2	MCZ-(Lerbekmo)			X	X			47°35′48.06″N	106°26′6.84″W
HC-1AD	MCZ-(Lerbekmo)	66.003 ± 0.033	1/71	X		X		47°31′35.58″N	106°56′23.82″W
HX12-2	MCZ-(Lerbekmo)			X	X	X		47°38′49.80″N	106°33′37.14″W
U-11	MCZ-(Lerbekmo)			X				47°33′19.14″N	106°52′7.38″W
ZL12-1	MCZ-(Lerbekmo)			X	X	X		47°36′37.26″N	106°12′37.74″W
HC14-1	MCZ-(Lerbekmo)			X	X			47°31′35.58″N	106°56′23.82″W
HF-3AD	HFZ	65.990 ± 0.032	0/43		X			47°31′30.12″N	107°11′59.22″W
HF-3PR	HFZ	65.990 ± 0.032		X	X		X	47°31′30.24″N	107°11′59.52″W
HH12-2	HFZ	65.962 ± 0.026	1/78	X	X	X	X	47°32′23.16″N	107°10′16.62″W
GC12-2	Y	65.677 ± 0.041	125/243	X	X		X	47°30′57.60″N	107°4′6.06″W
GC12-3	Y	65.741 ± 0.022	2/106		X		X	47°30′57.60″N	107°4′6.06″W
HC13-1	Y				X		X	47°30′57.66″N	106°56′11.64″W
HH13-1	Y				X		X	47°32′4.98″N	107°10′7.38″W
HH13-2	Y			X	X		X	47°32′4.98″N	107°10′7.38″W
HH13-3	Y			X			X	47°31′20.22″N	107°10′39.12″W
IS13-2	Y						X	47°39′56.58″N	106°30′7.08″W
JC13-1	Y						X	47°36′20.40″N	106°12′37.62″W
JC13-2	Y			X			X	47°36′16.86″N	106°12′29.34″W
JC13-3	Y						X	47°36′16.92″N	106°12′30.78″W
JC13-4	Y				X		X	47°36′16.92″N	106°12′30.78″W
MK12-1	Y			X				47°35′51.84″N	107°20′24.84″W
MK13-1	Y						X	47°35′38.64″N	107°19′36.30″W
MC11-3	X	65.491 ± 0.032	0/53	X	X			47°37′47.50″N	106°10′12.40″W
HTC12-1	W	65.197 ± 0.024	1/86		X		X	47°11′55.68″N	107°23′7.26″W
SS11-3	W	65.118 ± 0.024	0/68		X		X	47°30′36.62″N	107°4′50.64″W
BB12-1	V	65.041 ± 0.023	0/175	X				47°29′21.84″N	107°4′23.82″W
BB11-1	U	64.866 ± 0.023	0/119				X	47°29′13.08″N	107°4′7.64″W
HTC12-3	U	64.904 ± 0.026	1/72					47°11′37.74″N	107°24′6.06″W

[a]Age and proportion of xenocrysts defined by $^{40}Ar/^{39}Ar$ data [*Renne et al.*, 2013; *Sprain et al.*, 2014]. Uncertainties are at the 1σ level and do not include systematic errors (See Sprain et al., 2014 for details).

need only to be mounted in standard epoxy grain mounts and polished to a relatively flat surface and several individual grains can be characterized in as little as an hour.

3.3. Pb IC Measurements

Lead ICs were measured on polished grain mounts by laser ablation multicollector inductively coupled plasma mass spectrometry at the Berkeley Geochronology Center. The technique employed ~110 μm diameter spots sizes and mass bias was corrected by sample-standard-bracketing relative to NIST SRM 612 glass. Based on the relative intensities of Pb ion beams between samples and reference materials, we estimate that they have approximately 5–20 ppm Pb. Other analytical details are presented in the supporting information.

3.4. Multidimensional Scaling

In order to reduce the effective dimensionality and highlight compositional differences and similarities between samples, we have applied multidimensional scaling to the elemental and isotopic compositions of

sanidine. Multidimensional scaling (MDS) takes a measure of dissimilarities, transforms them through principal component analysis (PCA), and returns a set of points whose distance from one another is proportional to their compositional similarities (for a discussion of MDS and PCA applied to geologic data sets, see *Vermeesch* [2013]). The result of MDS is a bivariate plot in which compositionally similar samples plot close together and compositionally dissimilar samples plot far apart. A detailed discussion of the methodology applied to the current data set is provided in the supporting information.

4. Results and Discussion

4.1. Mineral Chemistry and Pb Isotopic Compositions of Unique Bentonite Beds

Below, we describe the mineral chemistry and Pb ICs of bentonite beds in the Hell Creek region, some of which we interpret to be the products of the same eruptive event, and are therefore isochronous chronostratigraphic markers. The results are plotted in Figure 4 and in tables in the supporting information. These interpretations are based on currently available data, but we expect that they may evolve over time as new data become available.

The MDS diagram (Figure 5) places a first-order constraint on the topology of the compositional variations and displays a good separation between groups of samples. In this plot, the magnitude of the first MDS vector (the *x* axis) largely reflects differences in the Pb ICs and the magnitude of the second MDS vector (the *y* axis) largely reflects differences in chemical composition. Four main groups are highlighted, with the stratigraphic context and compositional details outlined below. A unique group defined by W-coal bentonites occurs at the top of the diagram, characterized by an unusual chemical composition. Three unique compositions can be distinguished in bentonite samples from Z coals, which have wide E-W variations and subtle N-S variations. Samples of Y-coal bentonites are dispersed, but mainly form a group intermediate between the groups from the bentonites in the Z-suite coal beds. Notably, samples HH13-2 and HH13-3, which were taken from the same bentonite at different sites separated by ~1.3 km, plot in similar locations near the lower right-hand corner of the plot. The dispersion in these two samples (particularly in the second MDS vector) can be mainly attributed to the unusual variability in the compositions of the feldspars, probably reflecting varying degrees of magma mixing or assimilation prior to eruption (see below for details).

4.1.1. Bentonite Beds in Z-Suite Coals

One of the most important stratigraphic horizons in this region is the so-called Z coal, which marks the boundary between the Hell Creek Formation and the overlying Fort Union Formation. Like many of the other named coal units, the "Z coal" is a complex of lignite beds with variable lateral continuity that occur within a narrow stratigraphic range [*Collier and Knechtel*, 1939]. Following *Sprain et al*. [2014] and *Swisher et al*. [1993], we recognize three important Z coals: the IrZ, the HFZ, and the MCZ.

The IrZ is a particularly important unit, because it locally contains a spike in platinum group element concentrations and a thin clay layer that are both attributed to fallout from the Chicxulub impact associated with the end-Cretaceous extinction [*Alvarez*, 1983; *Smit and Van der Kaars*, 1984; *Baadsgaard et al*., 1988]. This coal is usually thin, varying between 4 and 20 cm thick. A bentonite layer preserved in the IrZ coal, occurring several cm above the marker horizon correlated with the impact, provides the best geochronological control on the timing of this event and is used as the best estimate of the age of the K-Pg boundary, currently estimated at 66.043 Ma [*Renne et al*., 2013; *Sprain et al*., 2014]. This bentonite has been tentatively identified and sampled at five localities: Hell Hollow, Hauso Flats, Nirvana, Snow Creek Road, and McKeever (Figure 1). At each locality the bentonite is thin (0.1–0.4 cm), pink, sanidine-bearing, and located 1–3 cm above the impact layer.

The Hauso Flats Z (HFZ) coal is a coal only present in the western Williston basin. The HFZ coal occurs 15–20 m above the IrZ coal, with an age of 65.973 Ma, approximately 70 ka younger than the KPB as defined by the IrZ coal [*Sprain et al*., 2014]. The HFZ coal is unusually thick, often varying between 1.5 and 3 m. This unit provides a constraint on the age of the Puercan 1 faunal range, and therefore a crucial constraint on the tempo of post KPB recovery. In this coal, two distinct bentonites stand out. The lowermost bentonite layer is thin (~0.5–1.0 cm), red, and contains sanidine. A distinctive feature of this bentonite is the presence of coarse pseudomorphs of cuspate glass shards. The second bentonite occurs ~10 cm above the first. It has a similar red color, is ~5 cm thick, and contains coarsely crystalline, euhedral sanidine and biotite

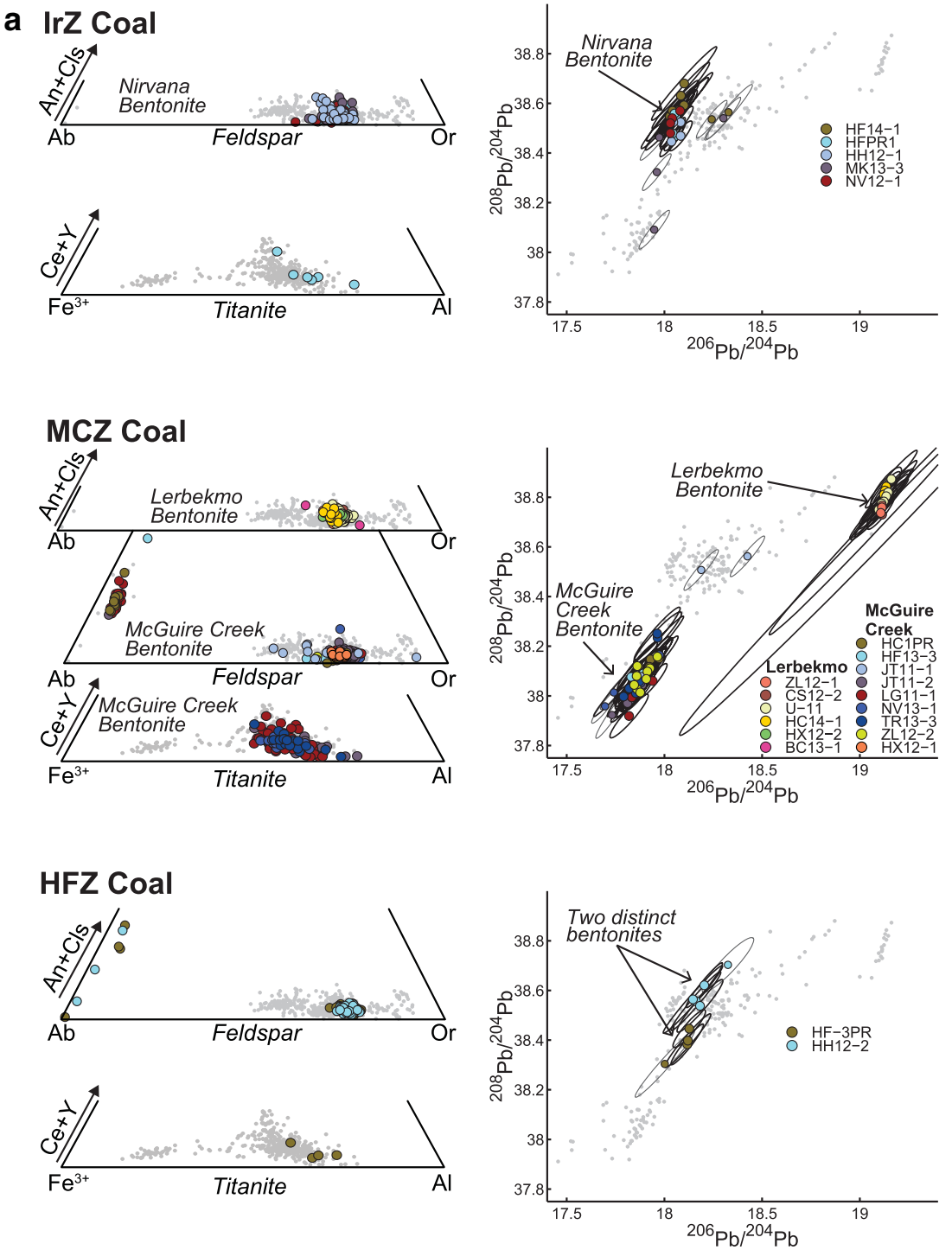

Figure 4. Compositional data for feldspar grains from bentonite samples from the (a) Z-complex and (b) all other coals. (left column) truncated ternary diagrams for feldspar and titanite. The feldspar diagrams plot the relative abundances of the orthoclase (Or), albite (Ab) and sum of the anorthite (An) and celsian (Cls) components, and the titanite diagrams plot the relative molar abundances of Fe^{3+}, Al, and the sum of Ce+Y. The celsian component is small for most of the feldspar compositions shown here. Samples CS12-2, ZL12-1, HC13-1, and GC12-2 each have a single analyzed grain of plagioclase feldspar, which have been omitted from the ternary diagrams for clarity. The uncertainties are generally smaller than the size of the symbols. (right column) the diagrams on the right plot the Pb isotope compositions of feldspar grains, with uncertainty ellipses plotted at 95% confidence. For those samples that have a clear central group with outliers, those analyses interpreted as xenocrysts (and therefore not representing the isotopic composition of the juvenile material in the bentonite) are deemphasized by using a thinner line and smaller symbols.

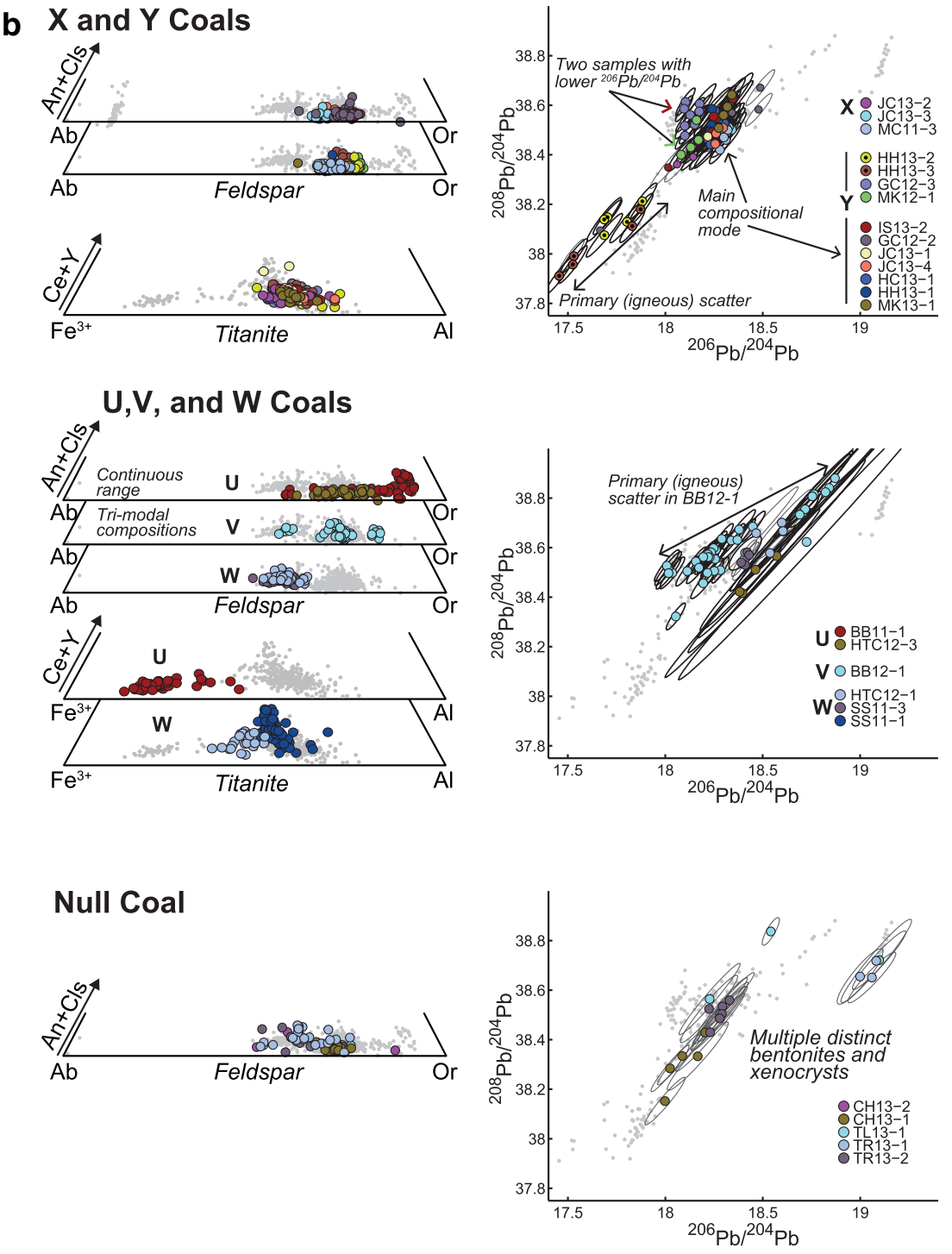

Figure 4. (continued)

crystals. Based on stratigraphic height, coal thickness, and identification of bentonites, the HFZ coal has been identified at two localities: Hauso Flats and Hell Hollow.

In the eastern portion of the area shown in Figure 1 (i.e., east of the Flag Butte section), there has not yet been an identification of Ir-concentration spikes or other indication of an impact horizon. In this region, *Lofgren* [1995] and *Wilson* [2014] determined that the lignite best fitting the definition of the

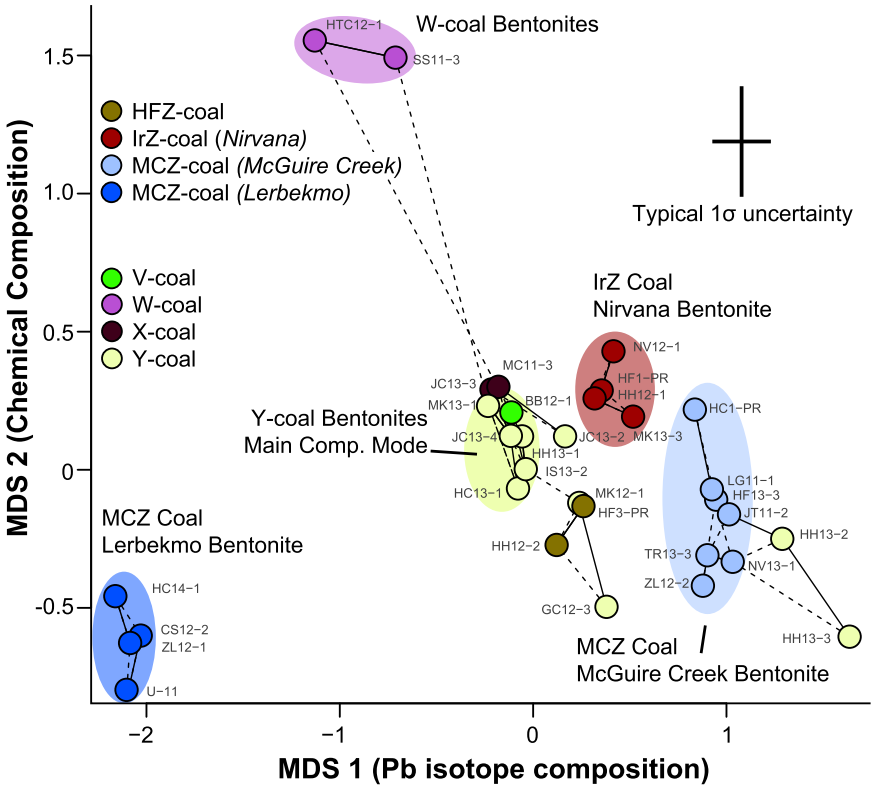

Figure 5. Multidimensional scaling plot of the combined chemical and isotopic data. The compositional distance represented by the *x* axis is dominated by variation in Pb isotope composition and the compositional distance in the *y* axis is dominated by the variation in the chemical composition. The sample from the U-coal (HTC12-3) plots far from the range of these samples and is not included in this plot. The solid tie lines represent links between closest pairs, and the dashed tie lines represent links between the second closest pairs. The colored ellipses highlight some important compositional groups, but the size and shape of the ellipses have no quantitative meaning.

lithostratigraphic boundary between the Fort Union and Hell Creek Formations is present above the first appearance of Paleocene pollen [see also *Hotton*, 2002]. Informally, this unit is called the McGuire Creek Z coal (MCZ), named for its identification and pervasive outcropping in the McGuire Creek drainage [*Lofgren*, 1995]. The paleontological observations documented the diachroneity of the lithostratigraphic formational boundary and are consistent with the absence of impact indicators in this bed. Importantly, this unit provides a lower limit on the age of Puercan 1 fauna in the eastern basin [*Wilson*, 2013]. The MCZ appears to usually contain a distinctive pair of bentonites consisting of a thin lower layer and a thick upper layer. The thin lower layer is generally 0.5 to 2.5 cm thick, pink, and contains abundant coarse sanidine crystals. The thick upper layer varies between 5 and 10 cm in thickness, is most often gray-green in color, contains sanidine and biotite, and has a distinctive waxy texture. Typically 10–30 cm of coal separates the two bentonites. This couplet has been identified in three localities in the easternmost area of Figure 1: Z-line, McGuire Creek, and Bug Creek. Bentonites of similar character appear to occur in coal beds in the central and western portions of the area of Figure 1: Snow Creek Road, Lerbekmo, Flag Butte, Jared's Trike, Haxby Road, and Thomas Ranch, raising the possibility that they may be a regionally extensive feature that can be correlated across the region and link the stratigraphy of both areas. In some sections (e.g., Nirvana) only one of the bentonites is present in the MCZ, and in others, like Jared's Trike, additional bentonites are found. Bentonites from the MCZ yield a pooled age of 66.013 ± 0.044 Ma (1σ) [*Sprain et al.*, 2014].

The feldspar and titanite mineral chemistry and Pb isotopic compositions from several of these bentonites distinguish three unique compositions that can be identified at multiple localities (Figure 5). A fourth cluster of data on the MDS diagram is shown below to be two different bentonite beds. These units are described here.

4.1.1.1. Nirvana Bentonite

The mineral chemistry and Pb IC from bentonite beds from five different IrZ coal localities (McKeever Ranch, Hauso Flats, Nirvana, Snow Creek Road, and Hell Hollow) are consistent with derivation from the same

eruptive event, and we term this the Nirvana Bentonite, named after the type locality at the Nirvana section, described in detail in the supporting information. The sanidine is intermediate in composition compared to other locations regionally. Although *Swisher et al*. [1993] analyzed a significant number of plagioclase grains, the samples studied here lack plagioclase. Titanite in bentonite at Hauso Flats has Ce+Y-Fe-Al compositions similar to titanite from other regional bentonites. The Pb ICs for four of the five samples form a cluster with a mean $^{206}Pb/^{204}Pb$ ~18.1. While there is little difference in the $^{206}Pb/^{204}Pb$ or $^{207}Pb/^{204}Pb$, there is scatter in the $^{208}Pb/^{204}Pb$ beyond that expected from the expanded analytical uncertainties. Four analyses from the McKeever Ranch sample and two from the Snow Creek Road sample yielded compositions distinct from the main mode, and are interpreted to be detrital contaminants. The combined compositional means and Pb ICs form a well-defined group on the MDS diagram.

4.1.1.2. Lerbekmo and McGuire Creek Bentonites

As described above, the MCZ can often be distinguished by the presence of two bentonite beds [*Sprain et al*., 2014], that were termed Z_1 and Z_2 at the Lerbekmo site by *Renne et al*. [2013] for lower and upper bentonite, respectively. We name these distinctive units Lerbekmo (the thick upper bentonite) and McGuire Creek (the thin lower bentonite), after their type localities at the Lerbekmo (also called the Hell Creek Road locality) and McGuire Creek sites. These localities are described in detail in the supporting information. Samples from beds tentatively correlated with the McGuire Creek bentonite were collected from the Snow Creek Road, Jared's Trike, McGuire Creek, Nirvana, Thomas Ranch, Haxby Road, and Z-line localities. At the Jared's Trike locality there appear to be two separate thin tuffs below a thick, Lerbekmo bentonite-like bed. Of these, sample JT11-1 has number of high and low-K feldspar grains, and a wide spread in Pb ICs that suggest the presence of detrital contamination. The other Jared's Trike sample (JT11-2) has a more restricted range in compositions consistent with other McGuire Creek bentonite-correlative samples. Samples from bentonite beds tentatively correlated with the Lerbekmo bentonite were collected from the Flag Butte, Z-line, Haxby Road, and the Lerbekmo localities. Feldspar from the McGuire Creek bentonite has a restricted range in compositions and the sample has abundant plagioclase. Titanite was observed in four of the bentonites displays consistently high Al relative to other titanite grains analyzed. Samples from the Lerbekmo bentonite have feldspar chemical compositions similar to the McGuire Creek bentonite but lack titanite. The Pb ICs from the McGuire Creek bentonite form a cluster with a narrow range in $^{206}Pb/^{204}Pb$ from 17.8 to 18.0. The two samples from the Jared's Trike locality and the sample from the Nirvana locality have a small amount of overdispersion, indicating the possible presence of xenocrysts. The four samples from the Lerbekmo bentonite have a small range at a relatively radiogenic $^{206}Pb/^{204}Pb$ of 19.1. The combined MDS analysis highlights their distinct Pb IC and subtle distinction in feldspar chemistry.

4.1.1.3. Unnamed Bentonite Beds From HFZ

Two bentonite beds from HFZ coals, one from Hauso Flats and another from Hell Hollow contain sanidine and plagioclase, the former displaying tight compositional range. Scarce titanite was observed in the bentonite at Hauso Flats. Feldspar chemical compositions have very little scatter and both samples have indistinguishable compositions. Although the Pb ICs are similar, the Hell Hollow sample has a slightly more radiogenic Pb IC. This is most easily seen in the $^{208}Pb/^{204}Pb$ results, where the Hauso Flats sample has a range from 38.30 to 38.45 and the Hell Hollow sample has a range from 38.54 to 38.70. These results confirm field observations that these are not the products of the same eruptive event, but the similarity in Pb IC may indicate that they are from the same or nearby eruptive center.

4.1.2. Bentonite Beds in X and Y-Suite Coals

Coal beds associated with the Y suite are poorly differentiated and often occur as multiple horizons in the same locality. This suite of coal beds is geologically more complex than the Z suite and includes more individual bentonite beds. From our collected bentonite samples, only one is from a mapped X coal [*Rigby and Rigby*, 1990] at the McGuire Creek locality in McCone county. While mapped as an X coal (defined as the second coal above the Z horizon), the stratigraphic position of this layer is similar to many mapped Y coals in Garfield county, thus we present the X and Y coals together. These suites of coals are associated with the Puercan 3 NALMA fauna and magnetic polarity chron boundary 29r/29n, making them an important potential set of marker horizons [e.g., *Clemens*, 2015].

The mineral chemistry measured by EPMA is generally nondistinct as plagioclase is scarce and the sanidine and titanite is similar in composition to that in bentonite beds in the Z-suite coals. This similarity is also reflected in the Pb ICs, which have a small amount of variability around a central composition. With the exception of the Hell Hollow samples (described below), bentonites from the X and Y-coal suites show the

presence of only 2–4 distinct Pb isotopic compositions, clustered around a $^{206}Pb/^{204}Pb$ of ~18.3 and $^{208}Pb/^{204}Pb$ ~36.5. They can be distinguished from the Nirvana bentonite, however, on the basis of a more radiogenic $^{206}Pb/^{204}Pb$. On the MDS plot, this homogeneity can be seen by the clustering of many mean values from Y-suite coal beds. Unfortunately, many of these beds are known or suspected to be different based on stratigraphic or paleomagnetic grounds, indicating that there are a number of different tephra with indistinguishable chemical and isotopic compositions.

4.1.2.1. Unnamed Assorted Bentonites

Several bentonite beds from Y-suite coals have similar compositions, including bentonite beds from Lerbekmo, Hell Hollow, Isaac Ranch, Jack's Channel, and McKeever Ranch. Some of the bentonite beds with indistinguishable compositions are clearly distinct bentonites; for example, sample HH13-1 and HH13-3 are unambiguously from different stratigraphic levels in the same continuous section. We therefore refrain from correlating any of these individual units throughout the area, and infer that they represent sequential eruptions from either a single volcanic center or region with similar compositions. This group has a Pb IC more radiogenic than those from the HFZ and the IrZ bentonites, with a $^{206}Pb/^{204}Pb$ of ~18.3. One of the Isaac Ranch samples is composed of only three analyses, one of which falls in the main mode range, but two of which have a $^{206}Pb/^{204}Pb$ above 19, in the same range as the MCZ-upper bentonite bed. The MDS of sanidine and Pb ICs and titanite data show HH13-2 and HH13-3 are different from the rest of the Y-Coals. HH13-1 appears to cluster with the others.

4.1.2.2. Unnamed Bentonite From Hell Hollow Y

The two samples from the upper Hell Hollow Y coal (HH13-2 and HH13-3) have a wide range in Pb IC, with a range in $^{206}Pb/^{204}Pb$ from 17.4 to 17.9, making them among the least radiogenic samples in the Hell Creek set. The samples themselves form a linear trend, oblique to the vector that defines a miss-correction for the ^{204}Hg interference and the vector for a miscorrection for mass bias, so we infer that the scatter represents real Pb IC heterogeneity. The trend is present but with some scatter in $^{206}Pb/^{204}Pb$ versus $^{208}Pb/^{204}Pb$ space to higher and lower $^{208}Pb/^{206}Pb$ values. Due to the strong linearity of the data, we interpret this trend as reflecting a real variability in the primary Pb ICs of the juvenile feldspar phenocrysts, probably due to open system processes in the source magmatic system such as magma mixing or crustal contamination [e.g., *Taylor*, 1980; *Ramos et al*., 2004].

4.1.2.3. Unnamed Bentonite Beds From Garbani Hill and McKeever Ranch

These two samples have slightly lower $^{206}Pb/^{204}Pb$ than the group of bentonites from the Y and X suites, and their Pb IC falls between the main Y-bentonites and the Nirvana bentonite. The two samples are close in composition, but can be distinguished on the basis of $^{208}Pb/^{204}Pb$, in which the average $^{208}Pb/^{204}Pb$ of the Garbani Hill sample is higher than the McKeever Ranch sample. The Garbani Hill sample is above the magnetostratigraphic polarity reversal and preliminary paleomagnetic work shows the McKeever Ranch sample is below the reversal (C. J. Sprain and P. R. Renne, unpublished data, 2015), confirming the inference from compositional data that they represent distinct volcanic events.

4.1.2.4. Garbani Hill Xenocrysts

A sample from the Garbani Hill locality (GC12-2) yielded scattered results, with the $^{206}Pb/^{204}Pb$ ranging from 17.5 to 19.1. Geochronological results from this sample [*Sprain et al*., 2014] reveal that nearly 50% of the sanidine grains from this sample are xenocrysts as old as 79 Ma, thus the scatter in the Pb results is easily interpreted as resulting from xenocrysts that were mixed with juvenile crystals during the eruptive, transport or depositional processes.

4.1.2.5. Bentonite Beds From the X Coal

It is difficult to differentiate between Y-suite coals and the X coal, in part because of the variable number of coals belonging to the Y suite in any given section. Sample MC11-3 is from a lignite mapped as the X coal by *Rigby and Rigby* [1990], but the criteria for this designation is unclear. The X coals are best described as the first coal beneath the W coal. Bentonite samples from a McGuire Creek X coal and a coal bed at the Jack's Channel locality above the Y coal containing main-mode-type bentonite have similarly nondistinct alkali feldspar compositions and nearly identical Pb ICs. They have a narrow range of Pb ICs with a mean $^{206}Pb/^{204}Pb$ of ~18.3, and a very close IC to the Y main mode, although can be distinguished by a lower average $^{208}Pb/^{204}Pb$ and $^{208}Pb/^{206}Pb$. At Jack's channel, a coal bed several meters above the X coal yields a bentonite that has a Pb IC that is similar, but extends to slightly less radiogenic values ($^{206}Pb/^{204}Pb \sim 18.05$).

4.1.3. Bentonite Beds in Null, U, V, and W Coals

We have characterized a number of bentonite beds from other lignite horizons in the region, including the Null, U, V, and W-coal suites. The Null coal is a Cretaceous unit that occurs in the Hell Creek Formation,

below the Z coal, and occurs within a few meters of the chron 29r paleomagnetic reversal (Sprain and Renne, unpublished data). Bentonites in the W coal provide a maximum age for the beginning of the Torrejonian NALMA in the study area, and the U coal marks the top of the Tullock Member. The V, and W coals represent other named coal units in the Tullock Member.

Bentonite beds from the Null coal. Bentonite beds from Null coals from three different localities were analyzed; two from the Cliff Hanger locality, one from the Tonstein Lignite locality, and two bentonite beds from a single lignite at the Thomas Ranch locality. The bentonites from all localities lack plagioclase and the alkali feldspar compositions showed a wide range of chemical variation. Titanite was observed at the Tonstein Lignite and Thomas Ranch localities and is similar in compositions to titanite from the Y and Z-suite coals. The two Thomas Ranch bentonite beds, samples from different portions of the same outcrop, have distinct Pb ICs, TR13-1 has a mean $^{206}Pb/^{204}Pb$ of ~18.3, whereas TR13-2 has a mean $^{206}Pb/^{204}Pb$ of 19.0. These are, in turn, distinct from the samples from Cliffhanger, which have $^{206}Pb/^{204}Pb$ that scatter narrowly around 18.0, and from Tonstein Lignite, which has widely scattered results. Geochronological results on a Null coal bentonite from Bug Creek show that >50% of the alkali feldspars analyzed were xenocrysts as old as 219 Ma [*Sprain et al*., 2014], likely the source of scatter observed in Pb ICs.

4.1.3.1. Bentonite Beds From the W Coal

There are three samples of bentonite from W coals, one from Horsethief Canyon and two from the Saddle Section, one from each of the pair of lignite beds making up the composite W "coal" at that locality. The two samples from which there are feldspar chemical data have the lowest observed orthoclase contents of the Hell Creek region feldspars. Although they have overlapping feldspar compositions, their Pb ICs are distinct: Sample SS11-3, from the upper coal within the W-coal doublet at Saddle section, forms a tight cluster at a $^{206}Pb/^{204}Pb$ of 18.4, whereas the main cluster of analyses from Horsethief Canyon sample HTC12-1 have a mean $^{206}Pb/^{204}Pb$ near 18.6. Titanite in the two samples from the Saddle Section is different from other samples regionally, as well as from one another. Sample SS11-1, from the lower coal within the W-coal doublet located at Saddle Section, has relatively high Ce+Y concentrations while HTC12-1 (mapped as the UW coal in *Archibald* [1982] at Horsethief Canyon) has compositions with intermediate Fe contents. Observed differences in chemistry corroborate with field evidence suggesting that SS11-1, SS11-3, and HTC12-1 are each unique bentonites within the W coal. SS11-1 samples a bentonite located near top of the lower coal within the W-coal doublet at the Saddle Section locality. SS11-3 was collected from a bentonite located near the top of the upper coal within the doublet, ~2 m above SS11-1. At Horsethief Canyon, sample HTC12-1 was collected from near the top of single thick (~1.5 m) coal, mapped as the UW [*Archibald*, 1982]. While mapped as a UW coal, this coal has been shown to correlate temporally with the W coal at the Saddle Section locality [*Sprain et al*., 2014], however $^{40}Ar/^{39}Ar$ results indicate that the ages of SS11-3 and HTC12-1 barely overlap at two sigma [*Sprain et al*., 2014], suggesting that these samples are not from the same bentonite. The coal is located at the bottom of the section and there is no evidence for a doublet at this locality.

4.1.3.2. Bentonite From the V Coal

The single sample from the V coal, BB12-1, has a $^{40}Ar/^{39}Ar$ age of 65.041 ± 0.048 Ma (1σ), about 1 Ma older than the K-Pg boundary [*Sprain et al*., 2014]. The sanidine from this sample has an unusually wide range in chemical composition exhibiting three distinct compositional modes. The results from the $^{40}Ar/^{39}Ar$ analyses indicate a bimodal distribution in Ca/K, despite the presence of only a single age population defined by the $^{40}Ar/^{39}Ar$ results. The wide range in chemical compositions is mirrored by a range in Pb ICs. The $^{206}Pb/^{204}Pb$ have a continuous range from ~18.0 to ~18.8, with a positive correlation between $^{206}Pb/^{204}Pb$ and both $^{207}Pb/^{204}Pb$ and $^{208}Pb/^{204}Pb$. The results can be divided into high and low Pb concentration groups. The high-Pb group has higher precision and forms the main body of the trend on the less radiogenic side. The low-Pb group, although results are imprecise, clearly have a more radiogenic $^{206}Pb/^{204}Pb$. A small number of analyses had intermediate Pb ICs and signal intensities—we infer that these analyses measured mixed zones between the low and the high [Pb] groups. The more radiogenic, low-Pb samples identified by laser ablation are associated with domains with low relative abundances of albite component, and there is a crude positive correlation between anorthite component and $^{206}Pb/^{204}Pb$ probably reflecting magma chamber processes.

4.1.3.3. Bentonite Beds From the U Coal

Two bentonite samples from the U coal, one from Horsethief Canyon (HTC12-3) and another from Biscuit Butte (BB11-1) were analyzed for both mineral chemistry and Pb ICs. Correlation of the two coals (cf. the

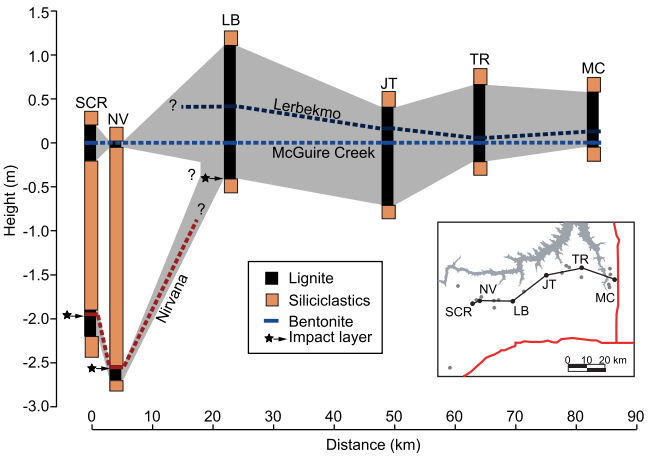

Figure 6. Fence diagram through selected sections of the Z-coal complex, showing relationships between the three distinctive bentonites and their host lignites. The SCR and NV sections represent the first documented stratigraphic relationship between McGuire Creek and Nirvana bentonites.

interbedded bentonites) is somewhat equivocal, and *Archibald* [1982] designated the Horsethief Canyon unit as the U coal. Feldspar and titanite from both samples displayed compositions distinctly different from bentonites in other coal horizons. Plagioclase was not observed and sanidine exhibits a range of compositions with the highest Or contents observed regionally. Titanite was found in bentonite from Biscuit Butte and displays compositions with uniquely high Fe contents. Both samples had small grains and relatively low Pb concentrations, compromising the quality of the analytical results. The sample from Horsethief Canyon has low-precision results, but the analyses have a mean $^{206}Pb/^{204}Pb$ of about 18.4. The sample from Biscuit Butte had low-precision results, which did not preclude correlation with the Horsethief Canyon sample, but were too low quality to report here.

4.2. Implications for the Tephrostratigraphy of the Hell Creek Region

Results presented here complement ongoing efforts to refine the chronostratigraphy of the KPB and recovery interval in the Hell Creek region. The new bentonite framework provides a more accurate stratigraphic scheme than one based on coals, which has many drawbacks. Of particular significance is the validation that the feldspar composition and Pb isotope systematics provide for correlation of bentonites in the Z suite of lignite horizons. Within this stratigraphic interval, the results provide further justification for the pooling of ages from different localities to improve the precision of age estimates because they provide additional evidence that they are products of unique eruption events. Of particular note is confirmation that the Nirvana bentonite, which provides the best constraint on the age of the Cretaceous-Paleogene boundary, is the product of a single eruption. This information can potentially be used to help locate the KPB in areas where an Ir anomaly cannot be found—geochronological data can be of great use, but have a finite precision that (in the absence of compositional data) can result in significant ambiguities in placement of the KPB. In addition, the unique composition of the Lerbekmo and McGuire Creek bentonites from the MCZ coal allows them to be identified throughout the Hell Creek area, linking the MCZ coal in the eastern part of the area with the better understood stratigraphy in the western area, potentially providing better constraints on the age of Puercan 1 NALMA fauna.

The prospects for utilizing these techniques to unravel the complicated stratigraphy of the Y suite of coals are more limited. Despite some variability, the compositional similarity between bentonite beds that are known to be distinct, i.e., are superposed in a given stratigraphic section, limits the ability of this technique to provide unique correlations. The proportion of bentonites sampled from Y-suite lignites remains relatively small—for example, at the McKeever section the Y coal contains six probable bentonites, only one of which (MK12-1) was sampled. A higher density of sampling, particularly in single localities, may demonstrate more variability and provide a better framework, but the present state of knowledge is not sufficient for stratigraphic correlation.

Some unique compositions of bentonites located in the upper portions of the Tullock Member may assist future correlations. For example, the heterogeneous Pb ICs and multimodal bulk compositions from the bentonite identified in the V coal are very distinctive, and should be easy to identify in other sections. Alkali feldspars and to some extent titanite can uniquely identify the U, V, and W-coal bentonites we have analyzed on the basis of EPMA data alone and are further enhanced by the incorporation of Pb ICs. The U coal marks the top of the Tullock Member and sanidine from the samples analyzed display the highest Or contents and titanite is unusually rich in iron. The V coal marks the C29n/C28r reversal [*LeCain et al.*, 2014] and sanidine grains from the interbedded bentonite are uniquely multimodal. The W coal occurs near the

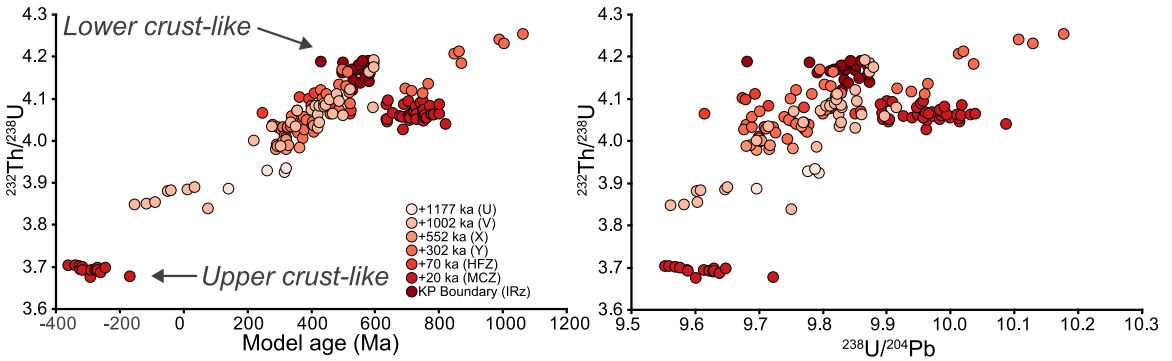

Figure 7. Plot of relative U, Th, and Pb abundances, and separation time, that are required to achieve the Pb isotope compositions measured in this study in a single separation event from a Stacey and Kramers-like geochemical reservoir [*Stacey and Kramers*, 1975; *Albarède et al*., 2012].

beginning of the Torrejonian NALMA and the samples analyzed have alkali feldspar with the highest albite component and titanite with the highest Ce+Y concentrations. As with the Y-suite coals, we have only analyzed a small proportion of the bentonites present in the W coals, where dozens of possible bentonites have been counted in a typical doublet spanning ~3 m. Further work will be required to characterize the compositional space defined by bentonites of this interval.

The identification of unique bentonites in lignites, especially in the Z-complex, serves as an unequivocal means to establish the aerial extent of lignite forming environments at specific times. This is highlighted by the cross section in Figure 6, illustrating the complex relationship between the near-KPB lignites in the western and the eastern portions of the Hell Creek region. With sufficiently dense sampling, this could be used for mapping out distinct facies' distributions and their changes over time, to great benefit in deciphering paleoecological evolution. However, it remains to be established whether a given bentonite eruption is recorded ubiquitously in all coal-forming environments available at the time of the eruption.

4.3. Sources

Lead ICs can be characterized by model ages and compositions, representing the U-Th-Pb systematics and reservoir "age" necessary to obtain the present-day compositions after a single stage separation from a

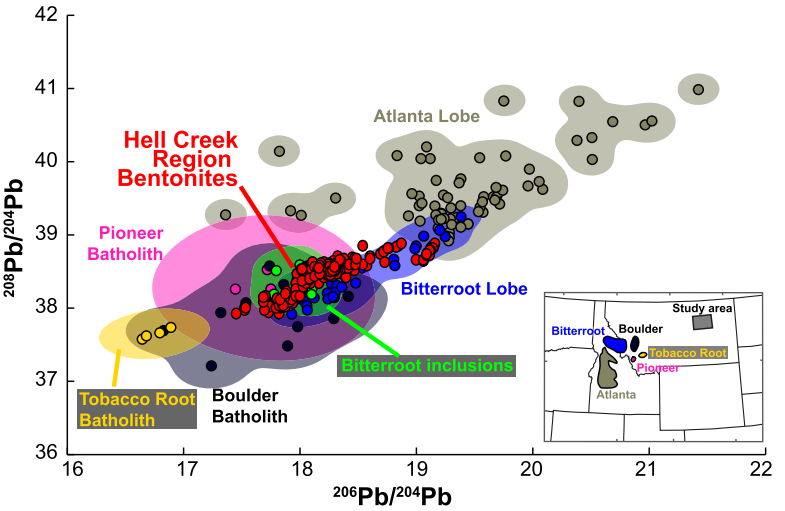

Figure 8. Plot of Pb isotope compositions of Hell Creek region bentonites (red circles) and the available Pb isotope compositions of nearby and approximately contemporaneous igneous rocks (with data from *Shuster and Bickford* [1985]; *Norman and Leeman* [1989]; *Clarke* [1990]; *Gunn* [1991]; *Toth and Stacey* [1992]; *Doe and Sanford* [1995]; *Panneerselvam et al*. [2006]; *Unruh et al*. [2008]; *Gaschnig et al*. [2012]). The inset figure is a schematic map of the location of these plutonic rocks relative to the Hell Creek region (modified from *Gaschnig et al*. [2012, 2013]).

model reservoir (Figure 7) (for details, see *Albarède et al*. [2012]). The lower continental crust has a uniquely high model κ value ($^{232}Th/^{238}U$) due to the common occurrence of U-loss via partial melting in the lower crust [e.g., *Zartman and Doe*, 1981]. The bulk of the data have relatively high values of κ and ca. 500 Ma model ages (Figure 8), suggesting the strong presence of ancient lower crust in the volcanic sources. This array projects toward a small group of data with more typical modern upper crustal composition, including near-zero model ages and lower κ values—a group mainly represented by the near-KPB Lerbekmo bentonite and the Cretaceous aged samples TR13-1.

The Pb ICs of feldspars from the tephra will match the Pb IC of their magmatic sources, so they can aid in determining the sources of the tuffs. Available Pb isotopic data from approximately KPB-aged igneous sources are plotted in Figure 8. Some previous workers have suggested that they can be traced to the Elkhorn Mountains volcanics [*Cherven and Jacob*, 1985], but these rocks are probably too old, as geological constraints make them older than the (largely) 80–74 Ma Boulder Batholith [*Tilling et al*., 1968; *Rutland et al*., 1989; *Thomas et al*., 1990; *Rogers et al*., 1993; *Roberts and Hendrix*, 2000; *Lund et al*., 2002]. Other plausible sources include the poorly dated Judith Mountains volcanics [*Zhang and Spry*, 1994] and more distally, any volcanism associated with the latest stages of the Boulder Batholith [*Lund et al*., 2002] or the earliest stages of the Bitterroot lobe of the Idaho Batholith [*Gaschnig et al*., 2010, 2012], which temporally straddles the KPB. The Pb ICs from the Hell Creek tephras are similar to measured values from both the Boulder Batholith and the Bitterroot lobe, but the overlap is better between Bitterroot, as both extend to higher $^{206}Pb/^{204}Pb$ than the Boulder Batholith.

5. Conclusions

Based on a large database of combined chemical and Pb isotope composition measurements of feldspar ($\pm$titanite), we have shown that these data are useful complementary or alternative criteria for the unique identification of tephra. In the Hell Creek region, there are several tephras located at or within $<$100 ka of the Cretaceous-Paleogene boundary that have unique compositions and can therefore be identified throughout the region. These composition-based correlations improve the local stratigraphic framework by linking bentonite beds preserved at different localities, and provides additional justification for the use of pooled radioisotopic ages from different localities. The analyses necessary to infer these correlations are relatively rapid and inexpensive compared with geochronological analyses, and provide substantially better (i.e., effectively infinite) age resolution.

This is the first large data set of Pb ICs applied to tephrostratigraphy. For samples that have large enough grains and high enough Pb concentration, a unique signature can commonly be defined by a relatively small (e.g., 4–5) number of analyses because many tephra appear to have a Pb IC that is homogeneous to the 0.1% level for $^{206}Pb/^{204}Pb$. In many cases, this precision should be sufficient to identify individual centers from volcanic fields [e.g., *Doe et al*., 1982]. Here there appears to be a particularly strong affinity for the Pb IC that makes up many bentonite horizons in the Y coal, but it is unclear how many individual eruptions this represents. Two bentonite beds show clear evidence of primary (magmatic) heterogeneity that can be identified and differentiated from the presence of xenocrysts by highly linear trends between different Pb isotope ratios.

Results of this study show that one lignite bed in the Z-coal complex, the MCZ coal of *Lofgren* [1995], was deposited isochronously 30 $\pm$18 ka after the KPB [*Sprain et al*., 2014], over a contiguous area at least 80 km in lateral dimension based on the occurrences of the McGuire Creek bentonite. In contrast, the distribution of IrZ coals containing the Nirvana bentonites, which was erupted within $\sim$1 ka after the KPB, was much more restricted and the correspondingly smaller region of low environmental energy, hence high preservation potential, may also explain the limited distribution of preserved impact markers such as Ir anomalies.

The Pb isotope data suggest that the tephras intercalated with Z-suite coals were erupted over $\sim$70 ka from at least two distinct sources, one of which persisted to produce the tephras in the Y and X-suite coals for the ensuing $\sim$300 ka. Tephras in the U, V, and W-coal suites likely were produced from at least one additional source over the next $\sim$300 ka. The specific locations of the eruptive centers are unknown, but the tephras' Pb isotope compositions are compatible with the Idaho or Boulder batholith, which contain plutons of approximately the appropriate age range.

Acknowledgments
The full data sets and descriptions of techniques can be found online in the supporting information. Funding support was provided by the Ann and Gordon Getty Foundation, the Esper S. Larsen Fund of the University of California, Berkeley, the Geological Society of America. We thank the Charles M. Russell Wildlife Refuge for assistance. The Neptune-*Plus* used for Pb isotope analyses was funded by NSF grant EAR-0930054. We gratefully acknowledge various contributions from A. Ahmadzai, W. Clemens, A. Deino, D. Fowler, N. Fylstra, A. Jaouni, W. *Mitchell*, R. Mundil, A. Tholt, G. *Wilson*, A. Tripathy, W. Sharp, R. Gaschnig, and N. McLean. Land access was kindly provided by the Engdahl, McKeever, Tharp, and Bliss families. Reviewers John Westgate and Steve Bergman are thanked for constructive comments on the manuscript.

References

Albarède, F., A.-M. Desaulty, and J. Blichert-Toft (2012), A geological perspective on the use of Pb isotopes in archaeometry, *Archaeometry*, *54*(5), 853–867, doi:10.1111/j.1475-4754.2011.00653.x.

Alvarez, L. W. (1983), Experimental evidence that an asteroid impact led to the extinction of many species 65 million years ago, *Proc. Natl. Acad. Sci. U. S. A.*, *80*(2), 627–642.

Archibald, J. D. (1982), A study of Mammalia and Geology across the Cretaceous-Tertiary boundary in Garfield County, Montana, 306 pp., University of California Press, Berkeley, Calif.

Archibald, J. D., et al. (2010), Cretaceous extinctions: Multiple causes, *Science*, *328*(5981), 973–973, doi:10.1126/science.328.5981.973-a.

Arens, N. C., and A. H. Jahren (2000), Carbon isotope excursion in atmospheric CO_2 at the Cretaceous-Tertiary boundary: Evidence from terrestrial sediments, *PALAIOS*, *15*(4), 314–322, doi:10.1669/0883-1351(2000)015<0314:CIEIAC>2.0.CO;2.

Arens, N. C., and A. H. Jahren (2002), Chemostratigraphic correlation of four fossil-bearing sections in southwestern North Dakota, *Geol. Soc. Am. Spec. Pap.*, *361*, 75–93, doi:10.1130/0-8137-2361-2.75.

Arens, N. C., A. Thompson, and A. H. Jahren (2014), A preliminary test of the press-pulse extinction hypothesis: Palynological indicators of vegetation change preceding the Cretaceous-Paleogene boundary, McCone County, Montana, USA, *Geol. Soc. Am. Spec. Pap.*, *503*, 209–227, doi:10.1130/2014.2503(07).

Baadsgaard, H., and J. F. Lerbekmo (1980), A Rb/Sr age for the Cretaceous-Tertiary boundary (Z coal), Hell Creak, Montana, *Can. J. Earth Sci.*, *17*(5), 671–673.

Baadsgaard, H., J. F. Lerbekmo, and I. McDougall (1988), A radiometric age for the Cretaceous–Tertiary boundary based upon K–Ar, Rb–Sr, and U–Pb ages of bentonites from Alberta, Saskatchewan, and Montana, *Can. J. Earth Sci.*, *25*(7), 1088–1097.

Baadsgaard, H., J. F. Lerbekmo, J. R. Wijbrans, C. C. Swisher, and M. Fanning (1993), Multimethod radiometric age for a bentonite near the top of the Baculites-Reesidei zone of southwestern Saskatchewan (Campanian Maastrichtian stage boundary), *Can. J. Earth Sci.*, *30*(4), 769–775.

Bercovici, A., D. Pearson, D. Nichols, and J. Wood (2009), Biostratigraphy of selected K/T boundary sections in southwestern North Dakota, USA: Toward a refinement of palynological identification criteria, *Cretaceous Res.*, *30*(3), 632–658, doi:10.1016/j.cretres.2008.12.007.

Bohor, B. F. (1990), Shocked quartz and more: Impact signatures in Cretaceous/Tertiary boundary clays, *Geol. Soc. Am. Spec. Pap.*, *247*, 335–342, doi:10.1130/SPE247-p335.

Bohor, B. F., E. E. Foord, P. J. Modreski, and D. M. Triplehorn (1984), Mineralogic evidence for an impact event at the Cretaceous-Tertiary boundary, *Science*, *224*(4651), 867–869, doi:10.1126/science.224.4651.867.

Borchardt, G. A., M. E. Harward, and R. A. Schmitt (1971), Correlation of volcanic ash deposits by activation analysis of glass separates, *Quat. Res.*, *1*(2), 247–260, doi:10.1016/0033-5894(71)90045-7.

Borchardt, G. A., P. J. Aruscavage, and H. T. Millard (1972), Correlation of the Bishop Ash: A Pleistocene marker bed, using instrumental neutron activation analysis, *J. Sediment. Res.*, *42*(2), 301–306, doi:10.1306/74D72527-2B21-11D7-8648000102C1865D.

Brown, F. H. (1982), Tulu Bor Tuff at Koobi Fora correlated with the Sidi Hakoma Tuff at Hadar, *Nature*, *300*(5893), 631–633, doi:10.1038/300631a0.

Brown, R. W. (1952), Tertiary strata in eastern Montana and western North and South Dakota, in *Billings Geological Society Guidebook: Third Annual Field Conference*, edited by F. P. Sonnenberg, pp. 89–92, Billings Geol. Soc., Billings, MT.

Calvert, W. R., C. F. Bowen, F. A. Herald, J. H. Hance, E. Stebinger, and A. L. Beekly (1912), Geology of certain lignite fields in eastern Montana, *U.S. Geol. Surv. Bull.*, *471*, 187–358.

Cherven, V. B., and A. R. Jacob (1985), Evolution of Paleogene depositional systems, Williston Basin, in response to global sea level changes, edited by M. R. Flores, and S. S. Kaplan, pp. 127–170, Cenozoic Paleogeography of the West-Central United States, Society of Economic Paleontologists and Mineralogists, Rocky Mountain Section, Denver, Colo.

Clark, J. D., et al. (2003), Stratigraphic, chronological and behavioural contexts of Pleistocene Homo sapiens from Middle Awash, Ethiopia, *Nature*, *423*(6941), 747–752, doi:10.1038/nature01670.

Clarke, C. B. (1990), The geochemistry of the Atlanta Lobe of the Idaho Batholith in the western United States, Cordillera, PhD thesis, Open Univ., Milton Keynes, U. K.

Clemens, W. A. (2015), Prodiacodon crustulum (Leptictidae, Mammalia) from the Tullock Member of the Fort Union Formation, Garfield and McCone Counties, Montana, USA, *PaleoBios*, *32*(1), 1–17.

Clemens, W. A., and J. H. Hartman (2014), From *Tyrannosaurus rex* to asteroid impact: Early studies (1901–1980) of the Hell Creek Formation in its type area, in *Through the End of the Cretaceous in the Type Locality of the Hell Creek Formation in Montana and Adjacent Areas, Geol. Soc. Am. Spec. Pap.*, vol. 503, edited by G. P. Wilson et al., pp. 1–87, Geological Society of America, Boulder, Colo.

Collier, A. J., and M. M. Knechtel (1939), The coal resources of McCone County, Montana, *U.S. Geol. Surv. Bull.*, *905*, 1–80.

Doe, B. R., and R. F. Sanford (1995), Lead isotope characteristics of ore systems in central Idaho, *U.S. Geol. Surv. Bull.*, *2064*, M1–M29.

Doe, B. R., W. P. Leeman, R. L. Christiansen, and C. E. Hedge (1982), Lead and strontium isotopes and related trace elements as genetic tracers in the Upper Cenozoic rhyolite-basalt association of the Yellowstone Plateau Volcanic Field, *J. Geophys. Res.*, *87*(B6), 4785–4806, doi:10.1029/JB087iB06p04785.

Fastovsky, D. E. (1987), Paleoenvironments of vertebrate-bearing strata during the Cretaceous-Paleogene transition, Eastern Montana and Western North Dakota, *PALAIOS*, *2*(3), 282–295, doi:10.2307/3514678.

Fastovsky, D. E., and R. H. Dott (1986), Sedimentology, stratigraphy, and extinctions during the Cretaceous-Paleogene transition at Bug Creek, Montana, *Geology*, *14*(4), 279–282, doi:10.1130/0091-7613(1986)14<279:SSAEDT>2.0.CO;2.

Folinsbee, R. E., H. Baadsgaard, and G. L. Cumming (1963), Dating of volcanic ash beds (bentonites) by the K-Ar method, *Nucl. Geophys.*, edited by P. M. Hurley, G. Faure, and C. Schnetzler, *1075*, pp. 70–82, National Academy of Sciences–National Research Council, Washington, D. C.

Fowler, C. M. R., and E. G. Nisbet (1985), The subsidence of the Williston Basin, *Can. J. Earth Sci.*, *22*(3), 408–415, doi:10.1139/e85-039.

Gaschnig, R. M., J. D. Vervoort, R. S. Lewis, and W. C. McClelland (2010), Migrating magmatism in the northern US Cordillera: In situ U–Pb geochronology of the Idaho batholith, *Contrib. Mineral. Petrol.*, *159*(6), 863–883, doi:10.1007/s00410-009-0459-5.

Gaschnig, R. M., J. D. Vervoort, R. S. Lewis, and B. Tikoff (2012), Isotopic evolution of the Idaho batholith and Challis intrusive province, northern US Cordillera, *J. Petrol.*, *52*, 2397–2429, doi:10.1093/petrology/egr050.

Gaschnig, R. M., J. D. Vervoort, R. S. Lewis, and B. Tikoff (2013), Probing for Proterozoic and Archean crust in the northern U.S. Cordillera with inherited zircon from the Idaho batholith, *Geol. Soc. Am. Bull.*, *125*(1–2), 73–88, doi:10.1130/B30583.1.

Gill, J. R., and W. A. Cobban (1973), Stratigraphy and geologic history of the Montana group and equivalent rocks, Montana, Wyoming, and North and South Dakota, *U.S. Geol. Surv. Prof. Pap.*, *776*, 37 pp.

Gunn, S. H. (1991), Isotopic constraints on the crustal evolution of southwestern Montana, PhD thesis, Univ. of Calif., Santa Cruz.
Hartman, J. H. (2002), Hell Creek formation and the early picking of the Cretaceous-Tertiary boundary in the Williston Basin, *Geol. Soc. Am. Spec. Pap.*, *361*, 1–7, doi:10.1130/0-8137-2361-2.1.
Hartman, J. H., R. D. Butler, M. W. Weiler, and K. K. Schumaker (2014), Context, naming, and formal designation of the Cretaceous Hell Creek Formation lectostratotype, Garfield County, Montana, in *Through the End of the Cretaceous in the Type Locality of the Hell Creek Formation in Montana and Adjacent Areas, Geol. Soc. Am. Spec. Pap. 503*, edited by G. P. Wilson et al., pp. 1–34, Geol. Soc. Amer., Boulder, Colo.
Hemming, S. R., and E. T. Rasbury (2000), Pb isotope measurements of sanidine monitor standards: Implications for provenance analysis and tephrochronology, *Chem. Geol.*, *165*, 331–337, doi:10.1016/s0009-2541(99)00174-6.
Hotton, C. L. (2002), Palynology of the Cretaceous-Tertiary boundary in central Montana: Evidence for extraterrestrial impact as a cause of the terminal Cretaceous extinctions, *Geol. Soc. Am. Spec. Pap.*, *361*, 473–501, doi:10.1130/0-8137-2361-2.473.
Housh, T., and S. A. Bowring (1991), Lead isotopic heterogeneities within alkali feldspars: Implications for the determination of initial lead isotopic compositions, *Geochim. Cosmochim. Acta*, *55*, 2309–2316, doi:10.1016/0016-7037(91)90106-f.
Kent, D. M., and J. E. Christopher (1994), Geological history of the Williston Basin and Sweetgrass arch, in *Geological Atlas of the Western Canada Sedimentary Basin*, pp. 421–429, Can. Soc. Pet. Geol. and Alberta Res. Counc., Calgary, AB.
LeCain, R., W. C. Clyde, G. P. Wilson, and J. Riedel (2014), Magnetostratigraphy of the Hell Creek and lower Fort Union Formations in northeastern Montana, *Geol. Soc. Am. Spec. Pap.*, *503*, 137–147, doi:10.1130/2014.2503(04).
Lipman, P. W., B. R. Doe, C. E. Hedge, and T. A. Steven (1978), Petrologic evolution of the San Juan volcanic field, southwestern Colorado: Pb and Sr isotope evidence, *Geol. Soc. Am. Bull.*, *89*(1), 59–82, doi:10.1130/0016-7606(1978)89<59:PEOTSJ>2.0.CO;2.
Lofgren, D. L. (1995), *The Bug Creek Problem and the Cretaceous-Tertiary Transition at McGuire Creek, Montana*, Univ. of Calif. Press, Berkeley, Calif.
Lowe, D. J. (2011), Tephrochronology and its application: A review, *Quat. Geochronol.*, *6*(2), 107–153, doi:10.1016/j.quageo.2010.08.003.
Ludwig, K. R., and L. T. Silver (1977), Lead-isotope inhomogeneity in Precambrian igneous K-feldspars, *Geochim. Cosmochim. Acta*, *41*(10), 1457–1471, doi:10.1016/0016-7037(77)90251-4.
Lund, K., J. N. Aleinikoff, M. J. Kunk, D. M. Unruh, G. D. Zeihen, W. C. Hodges, E. A. du Bray, and J. M. O'Neill (2002), SHRIMP U-Pb and 40Ar/39Ar age constraints for relating Plutonism and mineralization in the Boulder Batholith region, Montana, *Econ. Geol.*, *97*(2), 241–267, doi:10.2113/gsecongeo.97.2.241.
Mitchell, W. S., III (2014), High-resolution U-Pb geochronology of terrestrial Cretaceous-Paleogene and Permo-Triassic boundary sequences in North America, PhD thesis, Univ. of Calif., Berkeley.
Moore, J. R., G. P. Wilson, M. Sharma, H. R. Hallock, D. R. Braman, and P. R. Renne (2014), Assessing the relationships of the Hell Creek–Fort Union contact, Cretaceous-Paleogene boundary, and Chicxulub impact ejecta horizon at the Hell Creek Formation lectostratotype, Montana, USA, in *Through the End of the Cretaceous in the Type Locality of the Hell Creek Formation in Montana and Adjacent Areas, Geol. Soc. Am. Spec. Pap. 503*, edited by G. P. Wilson et al., pp. 1–14, Geol. Soc. Amer., Boulder, Colo.
Norman, M. D., and W. P. Leeman (1989), Geochemical evolution of Cenozoic-Cretaceous magmatism and its relation to tectonic setting, southwestern Idaho, U.S.A., *Earth Planet. Sci. Lett.*, *94*(1–2), 78–96, doi:10.1016/0012-821X(89)90085-X.
Panneerselvam, K., A. W. Macfarlane, and V. J. M. Salters (2006), Provenance of Ore metals in base and precious metal deposits of Central Idaho as inferred from lead isotopes, *Econ. Geol.*, *101*(5), 1063–1077, doi:10.2113/gsecongeo.101.5.1063.
Ramos, F. C., J. A. Wolff, and D. L. Tollstrup (2004), Measuring Sr-87/Sr-86 variations in minerals and groundmass from basalts using LA-MC-ICPMS, *Chem. Geol.*, *211*, 135–158.
Renne, P. R., A. L. Deino, F. J. Hilgen, K. F. Kuiper, D. F. Mark, W. S. Mitchell, L. E. Morgan, R. Mundil, and J. Smit (2013), Time scales of critical events around the Cretaceous-Paleogene boundary, *Science*, *339*(6120), 684–687, doi:10.1126/science.1230492.
Rigby, J. K., and J. K. Rigby Jr. (1990), *Geology of the Sand Arroyo and Bug Creek Quadrangles*, pp. 69–134, Dep. of Geol. Stud., Brigham Young Univ., McCone County, Mont.
Roberts, E. M., and M. S. Hendrix (2000), Taphonomy of a petrified forest in the two medicine formation (Campanian), Northwest Montana: Implications for Palinspastic restoration of the Boulder Batholith and Elkhorn Mountains Volcanics, *PALAIOS*, *15*(5), 476–482, doi:10.1669/0883-1351(2000)015<0476:TOAPFI>2.0.CO;2.
Rogers, R. R., C. C. Swisher III, and J. R. Horner (1993), 40Ar/39Ar age and correlation of the nonmarine two medicine formation (Upper Cretaceous), northwestern Montana, U.S.A., *Can. J. Earth Sci.*, *30*(5), 1066–1075, doi:10.1139/e93-090.
Rutland, C., H. W. Smedes, R. I. Tilling, and W. R. Greenwood (1989), Volcanism and Plutonism at Shallow Crustal Levels: The Elkhorn mountains volcanics and the Boulder Batholith, Southwestern Montana, in *Cordilleran Volcanism, Plutonism, and Magma Generation at Various Crustal Levels, Montana and Idaho Western Montana and Central Idaho*, edited by D. W. Hyndman et al., pp. 16–31, AGU, Washington, D. C.
Shuster, R. D., and M. E. Bickford (1985), Chemical and isotopic evidence for the petrogenesis of the northeastern Idaho Batholith, *J. Geol.*, *93*(6), 727–742.
Sinha, A. K. (1969), Removal of radiogenic lead from potassium feldspars by volatilization, *Earth Planet. Sci. Lett.*, *7*(2), 109–115, doi:10.1016/0012-821X(69)90022-3.
Smit, J. (1990), Meteorite impact, extinctions and the cretaceous-tertiary boundary, *Geologie En Mijnbouw*, *6*(2), 187–204.
Smit, J., and S. Van der Kaars (1984), Terminal Cretaceous extinctions in the Hell Creek area, Montana—Compatible with Catastrophic extinction, *Science*, *223*(4641), 1177–1179, doi:10.1126/science.223.4641.1177.
Smith, D. G. W., and J. A. Westgate (1968), Electron probe technique for characterising pyroclastic deposits, *Earth Planet. Sci. Lett.*, *5*, 313–319, doi:10.1016/S0012-821X(68)80058-5.
Sprain, C. J., P. R. Renne, G. P. Wilson, and W. A. Clemens (2014), High-resolution chronostratigraphy of the terrestrial Cretaceous-Paleogene transition and recovery interval in the Hell Creek region, Montana, *Geol. Soc. Am. Bull.*, *127*, 3(4), 393–409, doi:10.1130/B31076.1.
Stacey, J. S., and J. D. Kramers (1975), Approximation of terrestrial lead isotope evolution by a 2-stage model, *Earth Planet. Sci. Lett.*, *26*, 207–221.
Swisher, C. C., L. Dingus, and R. F. Butler (1993), $^{40}Ar/^{39}Ar$ dating and magnetostratigraphic correlation of the terrestrial Cretaceous-Paleogene boundary and Puercan Mammal Age, Hell Creek-Tullock formations, eastern Montana, *Can. J. Earth Sci.*, *30*, 1981–1996, doi:10.1139/e93-174.
Taylor, H. P., Jr. (1980), The effects of assimilation of country rocks by magmas on $^{18}O/^{16}O$ and $^{87}Sr/^{86}Sr$ systematics in igneous rocks, *Earth Planet. Sci. Lett.*, *47*(2), 243–254, doi:10.1016/0012-821X(80)90040-0.
Thomas, R. G., D. A. Eberth, A. L. Deino, and D. Robinson (1990), Composition, radioisotopic ages, and potential significance of an altered volcanic ash (bentonite) from the Upper Cretaceous Judith River Formation, Dinosaur Provincial Park, southern Alberta, Canada, *Cretaceous Res.*, *11*(2), 125–162, doi:10.1016/S0195-6671(05)80030-8.

Tilling, R. I., M. R. Klepper, and J. D. Obradovich (1968), K-Ar ages and time span of emplacement of the Boulder Batholith, Montana, *Am. J. Sci.*, *266*(8), 671–689, doi:10.2475/ajs.266.8.671.

Toth, M. I., and J. S. Stacey (1992), Constraints on the formation of the Bitterroot Lobe of the Idaho Batholith, Idaho and Montana, from U-Pb zircon geochronology and feldspar Pb isotopic data, *U.S. Geol. Surv. Bull.*, *2008*, 14 p.

Ukstins Peate, I., J. A. Baker, A. J. R. Kent, M. Al-Kadasi, A. Al-Subbary, D. Ayalew, and M. Menzies (2003), Correlation of Indian Ocean tephra to individual Oligocene silicic eruptions from Afro-Arabian flood volcanism, *Earth Planet. Sci. Lett.*, *211*(3–4), 311–327, doi:10.1016/S0012-821X(03)00192-4.

Ukstins Peate, I., J. A. Baker, M. Al-Kadasi, A. Al-Subbary, K. B. Knight, P. Riisager, M. F. Thirlwall, D. W. Peate, P. R. Renne, and M. A. Menzies (2005), Volcanic stratigraphy of large-volume silicic pyroclastic eruptions during Oligocene Afro-Arabian flood volcanism in Yemen, *Bull. Volcanol.*, *68*(2), 135–156, doi:10.1007/s00445-005-0428-4.

Unruh, D. M., K. Lund, M. A. Kuntz, and L. W. Snee (2008), Uranium-lead zircon ages and Sr, Nd, and Pb isotope geochemistry of selected plutonic rocks from western Idaho, *U.S. Geol. Surv. Open File Rep.*, 2008-1142, 37 pp.

Vermeesch, P. (2013), Multi-sample comparison of detrital age distributions, *Chem. Geol.*, *341*, 140–146, doi:10.1016/j.chemgeo.2013.01.010.

Westgate, J. A., N. J. G. Pearce, W. T. Perkins, P. A. Shane, and S. J. Preece (2011), Lead isotope ratios of volcanic glass by laser ablation inductively-coupled plasma mass spectrometry: Application to Miocene tephra beds in Montana, USA and adjacent areas, *Quat. Int.*, *246*, 82–96, doi:10.1016/j.quaint.2011.08.003.

Wilson, G. P. (2005), Mammalian faunal dynamics during the last 1.8 million years of the Cretaceous in Garfield County, Montana, *J. Mammalian Evol.*, *12*(1–2), 53–76, doi:10.1007/s10914-005-6943-4.

Wilson, G. P. (2013), Mammals across the K/Pg boundary in northeastern Montana, U.S.A.: Dental morphology and body-size patterns reveal extinction selectivity and immigrant-fueled ecospace filling, *Paleobiology*, *39*(3), 429–469, doi:10.1666/12041.

Wilson, G. P. (2014), Mammalian extinction, survival, and recovery dynamics across the Cretaceous-Paleogene boundary in northeastern Montana, in *Through the End of the Cretaceous in the Type Locality of the Hell Creek Formation in Montana and Adjacent Areas, Geol. Soc. Am. Spec. Pap. 503*, edited by G. P. Wilson et al., pp. 1–28, Geol. Soc. Amer., Boulder, Colo.

Zartman, R. E., and B. R. Doe (1981), Plumbotectonics—The model, *Tectonophysics*, *75*(1–2), 135–162, doi:10.1016/0040-1951(81)90213-4.

Zhang, X., and P. G. Spry (1994), Petrological, mineralogical, fluid inclusion, and stable isotope studies of the Gies gold-silver telluride deposit, Judith Mountains, Montana, *Econ. Geol.*, *89*(3), 602–627, doi:10.2113/gsecongeo.89.3.602.